Advances in Applied Mathematics and Mechanics
Adv. Appl. Math. Mech., Vol. **5**, No. 6, pp. 791-808

DOI: 10.4208/aamm.12-m12142
December 2013

A Solver for Helmholtz System Generated by the Discretization of Wave Shape Functions

Long Yuan[1] and Qiya Hu[2,*]

[1] *Academy of Mathematics and Systems Science, Chinese Academy of Sciences, Beijing 100190, China*
[2] *LSEC, Academy of Mathematics and Systems Science, Chinese Academy of Sciences, Beijing 100190, China*

Received 25 October 2012; Accepted (in revised version) 19 March 2013

Available online 6 September 2013

Abstract. An interesting discretization method for Helmholtz equations was introduced in B. Després [1]. This method is based on the ultra weak variational formulation (UWVF) and the wave shape functions, which are exact solutions of the governing Helmholtz equation. In this paper we are concerned with fast solver for the system generated by the method in [1]. We propose a new preconditioner for such system, which can be viewed as a combination between a coarse solver and the block diagonal preconditioner introduced in [13]. In our numerical experiments, this preconditioner is applied to solve both two-dimensional and three-dimensional Helmholtz equations, and the numerical results illustrate that the new preconditioner is much more efficient than the original block diagonal preconditioner.

AMS subject classifications: 65F08, 65N55

Key words: Helmholtz equation, ultra weak variational formulation, wave shape functions, preconditioner, iteration counts.

1 Introduction

A wide range of physical problems (for example, the acoustic scattering) in steady-state oscillation can be characterized using the Helmholtz equation (i.e., harmonic wave problem). Yet the main difficulties in numerically solving harmonic wave problems lie in the non-coercive nature of the problem and in the fact that the solution is oscillatory with a wavelength $\lambda=2\pi/\omega$. There exist many numerical methods for solving Helmholtz equation in literature: finite volume [2] and finite difference methods [3], the finite element

*Corresponding author.
Email: yuanlong@lsec.cc.ac.cn (L. Yuan), hqy@lsec.cc.ac.cn (Q. Y. Hu)

method (FEM) [4, 5], the Galerkin least-squares FEM [6], the quasi-stabilized finite element method [7], the Partition of Unity Method (PUM) [8,9], and the predefined reduced bases [10], the boundary element method (BEM) [11, 12] and the wave shape functions method [1, 13–15]. Among these methods, the last one becomes popular in the recent years.

The UWVF method was first proposed for solving Helmholtz equation and Maxwell equations by Cessenat and Després, see [1, 13, 16]. In this method, the Ultra Weak Variational Formulation is associated with a triangulation on the underlying domain where the trace of the analytic solution and its normal derivative on the skeleton of the mesh need to be computed. In the discrete UWVF, one uses exact solutions of the Helmholtz equation (without boundary condition) on every elements as basis functions, which are usually called *wave shape functions*. Once the discrete variational problem based on UWVF is solved, the full approximate solution can be obtained by solving local problems on the elements. It was proved in [1, 13] that the approximate solutions generated by the discrete UWVF possess the optimal error estimate. The results reported in the subsequent study [14] show that the method permits the use of a relatively coarse mesh and can reduce the numbers of DOFs per wavelength in comparison with the standard FEM.

Since the stiffness matrix associated with the UWVF method is of high ill condition when the frequency ω is large (so the mesh is fine), how to iteratively solve the system generated by the UWVF method is a difficult problem. Because of this, a block diagonal preconditioner $\mathcal{D}$ for the system generated by UWVF was proposed in [13]. In the numerical experiments of [13], the preconditioned Richardson's iteration with such block diagonal preconditioner is applied to solve the linear system generated by UWVF for some two-dimensional Helmholtz equations, and the numerical results indicate that the preconditioner $\mathcal{D}$ is slightly effective only. In the numerical experiments of [16], the authors adopt the preconditioned Bi-Conjugate Gradients Stabilized Method (BICGSTAB) with the above block diagonal preconditioner to solve the corresponding linear system since the BICGSTAB is faster than the Richardson's iteration. It was pointed out in [16] (pp. 743) that *an interesting question is how to obtain a better preconditioner than* $\mathcal{D}$. However, to our knowledge, up to now there is no better preconditioner proposed in literature.

In this paper we try to construct a more effective preconditioner than $\mathcal{D}$. Motivated by the domain decomposition method, we construct a coarse solver associated with a non-overlapping domain decomposition to the underlying domain. By adding the coarse solver into the original block diagonal preconditioner $\mathcal{D}$, we obtain a new preconditioner $\mathcal{B}$. We would like to emphasize that the new preconditioner is *not a standard* substructuring preconditioner based on non-overlapping domain decomposition, and is simple and easy to implement. To illustrate the effectiveness of the new preconditioner, we apply the preconditioned BICGSTAB method with the new preconditioner (and the original block diagonal preconditioner) to solve the systems generated by the UWVF method for both two-dimensional and three-dimensional Helmholtz equations. Numerical results show that the new preconditioner $\mathcal{B}$ is much more effective than the original block diagonal preconditioner $\mathcal{D}$. It is well known that a satisfactory theoretical result on a solver for

Helmholtz equations is difficult to obtain, so we do not consider this topic in the present paper.

The paper is organized as follows: In Section 2 we briefly recall the Ultra Weak Variational Formulation (UWVF) for Helmholtz equations. In Section 3, we describe discretization of the variational formulation. In Section 4, we construct a preconditioner for the stiffness matrix associated with the UWVF method. In Section 5, we report some numerical results to confirm the effectiveness of the new preconditioner.

2 Ultra weak variational formulation for Helmholtz equations

In this section we recall the Ultra Weak Variational Formulation (refer to [13]). Let Ω be a bounded and connected Lipschitz domain in $\mathbb{R}^l$ $(l=2,3)$. Consider Helmholtz equations which is formalized, normalizing the wave's velocity to 1, by

$$\begin{cases} -\Delta u-\omega^2 u=f, & \text{in } \Omega, \\ (\partial_{\mathbf{n}}+i\omega)u=t(-\partial_{\mathbf{n}}+i\omega)u+g, & \text{on } \gamma, \\ |t|<1, & t\in\mathbb{C}. \end{cases} \tag{2.1}$$

The outer normal derivative is referred to by $\partial_{\mathbf{n}}$ and the angular frequency by ω.

The basic idea of the ultra weak formulation is to consider a new unknown as well as a new continuous problem from which we will be able to go back to the original problem (2.1). To achieve this, let us consider a partition of Ω in the sense that

$$\begin{aligned} &\overline{\Omega}=\bigcup_{k=1}^{N}\overline{\Omega}_k, \quad \Omega_k\bigcap\Omega_j=\emptyset, \quad \text{for } k\neq j, \\ &\Gamma_{kj}=\partial\Omega_k\bigcap\partial\Omega_j, \quad \text{for } k\neq j, \\ &\gamma_k=\overline{\Omega}_k\bigcap\partial\Omega, \quad (k=1,\cdots,N), \\ &\gamma=\bigcup_{k=1}^{N}\gamma_k, \quad \Gamma=\bigcup_{k=1}^{N}\partial\Omega_k. \end{aligned}$$

In practice, the partition is a mesh of domain. The sets Ω_k are the elements. We denote a local interface by Γ_{kj} or a part of the boundary by γ_k. The size of the triangulation associated with the elements $\{\Omega_k\}$ is denoted by h.

2.1 Existence and uniqueness of the solution of (2.1)

The following classical result can be found in [1].

Theorem 2.1. *Let Ω be an open bounded set, and γ be its boundary assuming it is of class C^1 nearly everywhere. Let $f\in L^2(\Omega)$ and $g\in L^2(\Omega)$. We let $\zeta=(1-t)/(1+t)$ and assume t to be*

constant, $|t|<1$ *(then* $\Re(\zeta)>0$*). Then, there exists a unique* $u\in H^1(\Omega)$ *satisfying*

$$\begin{cases} \forall v\in H^1(\Omega) \\ \displaystyle\int_\Omega \nabla u\cdot\bar{\nabla}v-\omega^2\int_\Omega u\bar{v}+i\omega\zeta\int_\gamma u\bar{v}=\int_\Omega f\bar{v}+\frac{1}{1+t}\int_\gamma g\bar{v}, \end{cases} \tag{2.2}$$

or equivalently

$$\begin{cases} -\Delta u-\omega^2 u=f, & in\ \ \Omega, \\ (\partial_{\mathbf{n}}+i\omega)u=t(-\partial_{\mathbf{n}}+i\omega)u+g, & on\ \ \gamma. \end{cases} \tag{2.3}$$

2.2 Ultra weak variational formulation

Let $\mathbf{n}_k$ and $\partial_{\mathbf{n}_k}$ denote the outer normal vector and the outer normal derivative to $\partial\Omega_k$, respectively. Define

$$W(\partial\Omega_k)=\Big\{\psi_k=(-\partial_{\mathbf{n}_k}+i\omega)e|_{\partial\Omega_k}\in L^2(\partial\Omega_k);\ e\in H^1(\Omega_k),\ \Delta e+\omega^2 e=0\Big\},$$

and

$$W(\Gamma_h)=\prod_{k=1}^N W(\partial\Omega_k),$$

with the natural scalar product

$$(\varphi,\psi)_W=\sum_{k=1}^N\int_{\partial\Omega_k}\varphi_k\cdot\overline{\psi_k}ds,$$

hereafter $\varphi|_{\partial\Omega_k}=\varphi_k\in W(\partial\Omega_k)$, $\psi|_{\partial\Omega_k}=\psi_k\in W(\partial\Omega_k)$ and $\overline{\psi}$ denotes the complex conjugation of a complex function ψ, and

$$\Gamma_h=\prod_{k=1}^N\partial\Omega_k.$$

The value of the unknown φ in the UWVF formulation will be defined from the solution u of (2.1) as being

$$\varphi_k=((-\partial_{\mathbf{n}_k}+i\omega)u|_{\Omega_k})|_{\partial\Omega_k}.$$

For $\psi_k=(-\partial_{\mathbf{n}_k}+i\omega)e|_{\partial\Omega_k}\in W(\partial\Omega_k)$, with e satisfying $e\in H^1(\Omega_k)$ and $\Delta e+\omega^2 e=0$, we call such function $e=E_h^k(\psi_k)$ as the Helmholtz extension of ψ_k in Ω_k. Set $F_h^k(\psi_k)=(\partial_{\mathbf{n}_k}+i\omega)E_h^k(\psi_k)|_{\partial\Omega_k}$.

Theorem 2.2. *Let* $u\in H^1(\Omega)$ *be a solution of the Helmholtz problem* (2.1) *and satisfy the regularity hypothesis* $\partial_{\mathbf{n}_k}u\in L^2(\partial\Omega_k)$ *for any k. Then the boundary functions* $\varphi_k=((-\partial_{\mathbf{n}_k}+$

$i\omega)u|_{\Omega_k})|_{\partial\Omega_k}$ $(k=1,2,\cdots,N)$ *satisfy*

$$\sum_{k=1}^{N}\int_{\partial\Omega_k}\varphi_k\cdot\overline{\psi_k}ds-\Big(\sum_{k\neq j}\int_{\Gamma_{kj}}\varphi_j\cdot\overline{F_h^k(\psi_k)}ds+\sum_{k}\int_{\gamma_k}t\varphi_k\cdot\overline{F_h^k(\psi_k)}ds\Big)$$
$$=-2i\omega\sum_{k=1}^{N}\int_{\Omega_k}f\overline{E_h^k(\psi_k)}ds+\sum_{k=1}^{N}\int_{\gamma_k}g\overline{F_h^k(\psi_k)}ds,\quad\forall\psi=(\psi_1,\psi_2,\cdots,\psi_N)\in W(\Gamma_h).\tag{2.4}$$

Conversely, if $\varphi=(\varphi_1,\varphi_2,\cdots,\varphi_N)\in W(\Gamma_h)$ *is the solution of* (2.4)*, then the unique solution* u *of the original problem* (2.1) *can be defined by* $u|_{\Omega_k}=u_k$ *with* u_k *satisfying*

$$\begin{cases}-\Delta u_k-\omega^2u_k=f, & in\ \ \Omega_k,\\ (-\partial_{\mathbf{n}_k}+i\omega)u_k=\varphi_k, & on\ \ \Omega_k.\end{cases}\tag{2.5}$$

Proof. See [13]. □

Define the bilinear form

$$a(\varphi,\psi)=\sum_{k=1}^{N}\int_{\partial\Omega_k}\varphi_k\cdot\overline{\psi_k}ds$$
$$-\Big(\sum_{k\neq j}\int_{\Gamma_{kj}}\varphi_j\cdot\overline{F_h^k(\psi_k)}ds+\sum_{k}\int_{\gamma_k}t\varphi_k\cdot\overline{F_h^k(\psi_k)}ds\Big),\quad\varphi,\psi\in W(\Gamma_h).$$

Let $\xi\in W(\Gamma_h)$ be defined, via the Riesz representation theorem, by

$$(\xi,\psi)_W=-2i\omega\sum_{k=1}^{N}\int_{\Omega_k}f\overline{E_h^k(\psi_k)}ds+\sum_{k=1}^{N}\int_{\gamma_k}g\overline{F_h^k(\psi_k)}ds,\quad\forall\psi\in W(\Gamma_h).\tag{2.6}$$

Then the problem (2.4) is equivalent to

$$\begin{cases}\text{Find } \varphi\in W(\Gamma_h),\text{ such that}\\ a(\varphi,\psi)=(\xi,\psi)_W,\quad\forall\psi\in W(\Gamma_h).\end{cases}\tag{2.7}$$

3 Discretization of the variational formulation

In this section, we consider a discretization of the variational problem (2.7). The discretization is based on a finite dimensional space $W_p(\Gamma_h)\subset W(\Gamma_h)$. We first give the exact definition of a space $W_p(\Gamma_h)$.

3.1 The basis functions of $W_p(\Gamma_h)$

For convenience, when $f=0$ in (2.1), we call (2.1) a homogeneous problem. Otherwise, we refer to a nonhomogeneous problem. In each element Ω_k, we introduce a finite number of functions e_{kl} $(l=1,2,\cdots,p)$ supported in Ω_k and that are independent solutions of

the homogeneous Helmholtz equation (without boundary condition) in the element Ω_k ($k=1,2,\cdots,N$). To simplify, we consider some constant number p of basis functions for all elements Ω_k. Particularly, in this paper we will choose e_{kl} as the wave shape functions on Ω_k, which satisfy

$$\begin{cases} e_{kl}=e^{i\omega(\mathbf{x}\cdot\overrightarrow{\alpha_l})}, \\ \overrightarrow{\alpha_l}\cdot\overrightarrow{\alpha_l}=1, \\ l\neq m\to\overrightarrow{\alpha_l}\neq\overrightarrow{\alpha_m}, \end{cases} \tag{3.1}$$

where $\overrightarrow{\alpha_l}$ ($l=1,\cdots,p$) are unit wave propagation directions to be specified later.

Thus the space $W(\Gamma_h)$ is discretized by the subspace

$$W_p(\Gamma_h)=\left\{\psi_h\in W(\Gamma_h):\psi_h|_{\partial\Omega_k}=\sum_{l=1}^{p}\theta_{kl}(-\partial_{\mathbf{n}_k}+i\omega)e^{i\omega(\mathbf{x}\cdot\overrightarrow{\alpha_l})},\ \mathbf{x}\in\partial\Omega_k,\ \theta_{kl}\in\mathbb{C}\right\}. \tag{3.2}$$

It is clear that the basis functions of $W_p(\Gamma_h)$ can be defined as

$$\phi_{kl}(\mathbf{x})=\begin{cases} (-\partial_{\mathbf{n}_k}+i\omega)e_{kl}, & \text{on } \partial\Omega_k, \\ 0, & \text{on } \partial\Omega_j, \text{ satisfying } j\neq k, \end{cases} \quad (k,j=1,\cdots,N;\ l=1,\cdots,p). \tag{3.3}$$

During numerical simulations, the directions of the wave vectors of these wave functions, for two-dimensional problems, are uniformly distributed as follows:

$$\overrightarrow{\alpha_l}=\begin{pmatrix}\cos(2\pi(l-1)/p)\\ \sin(2\pi(l-1)/p)\end{pmatrix},\quad (l=1,\cdots,p).$$

For three-dimensional problems, the following formula proposed in [19] can be used to generate the wave propagation directions

$$\overrightarrow{\alpha}_{j1,j2,j3}=\frac{\overrightarrow{\hat{\alpha}}_{j1,j2,j3}}{\|\overrightarrow{\hat{\alpha}}_{j1,j2,j3}\|},\quad \overrightarrow{\hat{\alpha}}_{j1,j2,j3}=\begin{pmatrix}\tan((2j_1/n_t-1)\pi/4)\\ \tan((2j_2/n_t-1)\pi/4)\\ \tan((2j_3/n_t-1)\pi/4)\end{pmatrix},$$

where n_t is a given positive integer and $j_1,j_2,j_3=0,\cdots,n_t$ are positive integers chosen so that at least one of j_1, j_2, or j_3 is equal to zero or to n_t. Using this construction algorithm, the number of directions p becomes equal to $6n_t^2+2$. For example, choosing $n_t=2$, $n_t=3$, and $n_t=4$ leads to 26, 56 and 98 wave functions, respectively.

3.2 The discrete problem and the algebraic form of (2.7)

Let $W_p(\Gamma_h)$ be defined in the last subsection. Then the discrete variational problem associated with (2.7) can be described as follows:

$$\begin{cases} \text{Find } \varphi_h\in W_p(\Gamma_h), \text{ such that} \\ a(\varphi_h,\psi_h)=(\xi,\psi_h)_W,\quad \forall\psi_h\in W_p(\Gamma_h). \end{cases} \tag{3.4}$$

Let $\mathcal{A}$ be the stiffness matrix associated with the bilinear form $a(\cdot,\cdot)$ and the space $W_p(\Gamma_h)$, and let b denote the vector associated with the scalar product $(\xi,\psi_h)_W$. Namely, the entries of the matrix $\mathcal{A}$ are computed by $a_{k,j}^{l,m}=a(\phi_{jm},\phi_{kl})$; and the complements of the vector b are defined as $b_{k,l}=(\xi,\psi_{kl})_W$. Then the discretized problem (3.4) leads to the algebraic system below:

$$\mathcal{A}X=b, \tag{3.5}$$

where $X=(x_{11},x_{12},\cdots,x_{1p},x_{21},\cdots,x_{2p},\cdots,x_{N1},\cdots,x_{Np})^t\in\mathbb{C}^{pN}$ is the unknown vector.

After solving (3.5), we can get the solution φ_h of the problem (3.4). Furthermore, we can compute an approximation u_h of u. In practice, the discretized form of (2.5) is as follows:

$$\begin{cases} -\Delta\tilde{u}_h-\omega^2\tilde{u}_h=f, & \text{in } \Omega_k,\\ (-\partial_{\mathbf{n}_k}+i\omega)\tilde{u}_h=\varphi_h, & \text{on } \Omega_k. \end{cases} \tag{3.6}$$

Then any approximate solution of the above local equation can be regarded as $u_h|_{\Omega_k}$. In particular, when $f=0$ on Ω_k, the solution of the Eq. (3.6) can be obtained directly, i.e.,

$$u_h|_{\Omega_k}=\tilde{u}_h|_{\Omega_k}=\sum_{l=1}^{p}x_{kl}e_{kl},\quad (k=1,\cdots,N), \tag{3.7}$$

where x_{kl} and e_{kl} $(k=1,\cdots,N,\ l=1,2,\cdots,p)$ are defined by (3.5) and (3.1), respectively.

In general the system (3.5) is solved by some iterative method, for example, the preconditioned BICGSTAB method. Then we need to construct an efficient preconditioner $\mathcal{B}$ for the matrix $\mathcal{A}$, and use BICGSTAB method to solve the equivalent system

$$\mathcal{B}^{-1}\mathcal{A}X=\mathcal{B}^{-1}b. \tag{3.8}$$

4 A preconditioner for $\mathcal{A}$

4.1 The original preconditioner proposed in [13]

To iteratively solve the system (3.5), a block diagonal preconditioner was proposed in [13]. Let $\mathcal{D}$ denote the matrix associated with the scalar product in $W_p(\Gamma_h)$, and let $\mathcal{C}$ denote the matrix associated with the second part in the bilinear form $a(\varphi,\psi)$. Let ϕ_{kl} be the basis functions defined by (3.3). The exact definitions of them are given as follows (see [13] for the details):

i) The entries of the matrix $\mathcal{D}$ are defined by $d_{k,j}^{l,m}=(\phi_{jm},\phi_{kl})_W$, i.e.,

$$d_{k,j}^{l,m}==\delta_{kj}\int_{\partial\Omega_k}(-\partial_{\mathbf{n}_k}+i\omega)e_{jm}\overline{(-\partial_{\mathbf{n}_k}+i\omega)e_{kl}}. \tag{4.1}$$

ii) The entries of the matrix $\mathcal{C}$ are defined by $c_{k,j}^{l,m}=(\phi_{jm},\phi_{kl})_W-a(\phi_{jm},\phi_{kl})$, i.e.,

$$c_{k,j}^{l,m}=\begin{cases}\displaystyle\int_{\Gamma_{kj}}(\partial_{\mathbf{n}_k}+i\omega)e_{jm}\overline{(\partial_{\mathbf{n}_k}+i\omega)e_{kl}}, & \text{for } k\neq j,\\ \displaystyle\int_{\gamma_k}t(-\partial_{\mathbf{n}_k}+i\omega)e_{jm}\overline{(\partial_{\mathbf{n}_k}+i\omega)e_{kl}}, & \text{for } k=j.\end{cases}\tag{4.2}$$

It is easy to see that $\mathcal{D}$ is a block diagonal matrix. Then the matrix $\mathcal{A}$ can be written as

$$\mathcal{A}=\mathcal{D}-\mathcal{C}.\tag{4.3}$$

The matrix $\mathcal{D}$ was chosen as a preconditioner of $\mathcal{A}$ in [13]. From the numerical results reported in [13], we can see that the preconditioner $\mathcal{D}$ is slightly effective only.

4.2 A coarse subspace based on domain decomposition

We first coarsen the triangulation $\{\Omega_k\}$ as follows: let Ω be decomposed into the union of $D_1,D_2,\cdots,D_{n_0}$ such that D_r is just the union of several elements in $\{\Omega_k\}$ and satisfies

$$D_r\bigcap D_l=\emptyset,\quad \text{for } r\neq l.$$

Let d denote the size of the subdomains $D_1,\cdots,D_{n_0}$. Set

$$\Gamma_d=\bigcup_{r=1}^{n_0}\partial D_r\quad\text{and}\quad W_p(\Gamma_d)=\prod_{r=1}^{n_0}W_p(\partial D_r)$$

with

$$W_p(\partial D_r)=span\{\psi_{r1}(\mathbf{x}),\cdots,\psi_{rp}(\mathbf{x})\},$$

where

$$\psi_{rl}(\mathbf{x})=(-\partial_{\mathbf{n}}+i\omega)e^{i\omega(\mathbf{x}\cdot\overrightarrow{\alpha_l})}|_{\partial D_r},\quad \mathbf{x}\in\partial D_r,\quad (l=1,\cdots,p).$$

We try to design a solver associated with $W_p(\Gamma_d)$. Since $W_p(\Gamma_d)$ is not a subspace of $W_p(\Gamma_h)$, it can not be chosen as a coarse subspace of $W_p(\Gamma_h)$. In order to define a suitable coarse subspace of $W_p(\Gamma_h)$, we set $e_{rl}^d=e^{i\omega(\mathbf{x}\cdot\overrightarrow{\alpha_l})}$ $(\mathbf{x}\in D_r;\, l=1,2,\cdots,p)$ and define

$$\tilde{\phi}_{rl}=\begin{cases}(-\partial_{\mathbf{n}_k}+i\omega)e_{rl}^d, & \text{on } \partial\Omega_k, \text{ satisfying } \Omega_k\subset D_r,\\ 0, & \text{on } \partial\Omega_k, \text{ satisfying } \Omega_k\not\subset D_r,\end{cases}\qquad (r=1,\cdots,n_0;\ l=1,\cdots,p).\tag{4.4}$$

Then the desired coarse subspace can be defined as

$$\tilde{W}_p(\Gamma_d)=span\{\tilde{\phi}_{11},\cdots,\tilde{\phi}_{1p},\tilde{\phi}_{21},\cdots,\tilde{\phi}_{2p},\cdots,\tilde{\phi}_{n_01},\cdots,\tilde{\phi}_{n_0p}\}.$$

4.3 The new preconditioner

To describe the new preconditioner more clearly, we need to define a transformation matrix. With the basis functions defined in the last subsection, we define the transformation matrix $\mathcal{C}_d$ by

$$(\tilde{\phi}_{11}\cdots\tilde{\phi}_{1p}\tilde{\phi}_{21}\cdots\tilde{\phi}_{2p}\cdots\tilde{\phi}_{n_01}\cdots\tilde{\phi}_{n_0p})^t=\mathcal{C}_d(\phi_{11}\cdots\phi_{1p}\ \phi_{21}\cdots\phi_{2p}\cdots\phi_{N1}\cdots\phi_{Np})^t,$$

where $\{\phi_{kl}\}$ are the basis functions of $W_p(\Gamma_h)$ (see (3.3)).

Let $\mathcal{A}_d$ denote the stiffness matrix of the bilinear form $a(\cdot,\cdot)$ on the subspace $\tilde{W}_p(\Gamma_d)$. The matrix $\mathcal{A}_d$ can be viewed as a coarse solver associated with the non-overlapping domain decomposition described in the last subsection. It is easy to verify that $\mathcal{A}_d=\mathcal{C}_d\mathcal{A}\mathcal{C}_d^t$. Then the desired preconditioner $\mathcal{B}$ of $\mathcal{A}$ is defined as

$$\mathcal{B}^{-1}=\mathcal{D}^{-1}+\mathcal{C}_d^t\mathcal{A}_d^{-1}\mathcal{C}_d.$$

In applications we can make the domain decomposition such that $d\gg h$, so the order of $\mathcal{A}_d$ is much smaller than the order of $\mathcal{A}$. This means that the action of $\mathcal{B}^{-1}$ is cheap to implement (note that $\mathcal{D}$ is a block diagonal matrix).

5 Numerical experiments

In this section we apply the preconditioned BICGSTAB method with the preconditioners $\mathcal{D}$ and $\mathcal{B}$ to solve the system (3.5) generated by UWVF method for both two-dimensional and three-dimensional problems. In order to give a convincing conclusion, we also consider the damped preconditioned Richardson iteration with the preconditioner $\mathcal{D}$, where the damped factor β_n is chosen as 0.75 instead of a random variable (the number 0.75 seems almost the optimal damped factor). For simplicity, we will use "$\mathcal{B}$ (rep. $\mathcal{D}$)+BICGSTAB" to represent the preconditioned BICGSTAB method with the preconditioner $\mathcal{B}$ (rep. $\mathcal{D}$), and use "$\mathcal{D}$+Richardson" to represent the preconditioned Richardson iteration with the preconditioner $\mathcal{D}$. We report some numerical results to illustrate the efficiency of the new preconditioner $\mathcal{B}$.

In the examples tested in this section, we adopt a uniform triangulation $\mathcal{T}_h$ for the domain Ω as follows: Ω is divided into some small cubes (for three-dimensional case) or rectangles or triangles (for two-dimensional case) with the same size, where h denotes the length of the longest edge of the elements. In the two-dimensional case, the number p of basis functions in each element equals 12 (for the smooth case) or 7 (for the singular case). In the three-dimensional case, the number p of the basis functions in each element equals 26, which corresponds the positive integer n_t (defined in Subsection 3.1) being 2.

In order to determine the coarse solver $\mathcal{A}_d$ described in Subsection 4.2, we define subdomain D_r, $(r=1,\cdots,n_0)$ as follows: each subdomain (coarse element) D_r is a cube (for three-dimensional case) or rectangle (for two-dimensional case), which is just the union of several elements, and every subdomains D_r have the same size. Let d denote

the length of the longest edge of the subdomains D_r. In general we can define $d\approx\sqrt{h}$ in the domain decomposition method. However, we consider different choices of d in the following tests so that we can see how the iteration number and computing time depend on the different values of d/h. Note that the value d/h determines the number of the elements contained in each subdomain D_r, and so determines the number of the coarse elements D_r for a fixed fine mesh size h. Speaking more exactly, for a fixed h, when the value of d/h increases (so d increase), the number of the coarse elements D_r decreases and so the order of the matrix $\mathcal{A}_d$ decreases (but the iteration counts of $\mathcal{B}$+BICGSTAB increases).

The stopping criterion in the preconditioned BICGSTAB iteration is that the relative L^2-norm ϵ of the residual of the iterative approximation satisfies $\epsilon<1.0e-8$ (we choose initial guess $X_0=0$ in the iteration), and T_{sol} represents the computing time for solving the algebraic system (including the construction time of the preconditioner). To measure the accuracy of the resulting approximate solution u_h, we will use the relative L^2 norm

$$\text{err.}=\frac{\|u_{ex}-u_h\|_{L^2(\Omega)}}{\|u_{ex}\|_{L^2(\Omega)}}.$$

5.1 Wave propagation in a duct with rigid walls

The first model problem is the following Helmholtz equations for the acoustic pressure u and associated boundary conditions (see [20]):

$$\Delta u+\omega^2 u=0, \qquad \text{in } \Omega, \tag{5.1a}$$

$$\frac{\partial u}{\partial \mathbf{n}}=\cos(k\pi y), \qquad \text{on } x=0, \quad k\in\mathbb{N}, \tag{5.1b}$$

$$\frac{\partial u}{\partial \mathbf{n}}+i\omega u=0, \qquad \text{on } x=2, \tag{5.1c}$$

$$\frac{\partial u}{\partial \mathbf{n}}=0, \qquad \text{on } y=0,1, \tag{5.1d}$$

where $\Omega=[0,2]\times[0,1]$, and $\mathbf{n}$ denotes the outward boundary unit normal vector. The inlet boundary $x=0$ has an inhomogeneous Neumann condition, and the outlet boundary $x=2$ is characterized using an absorbing boundary condition. The boundaries $y=0,1$ are assumed to be perfectly rigid leading to vanishing normal derivatives on the boundary.

The exact solution to the problem can be obtained in the closed form as

$$u_{ex}(x,y)=\cos(k\pi y)(A_1e^{-i\omega_x x}+A_2e^{i\omega_x x}),$$

where $\omega_x=\sqrt{\omega^2-(k\pi)^2}$, and coefficients A_1 and A_2 satisfy the equation

$$\begin{pmatrix} \omega_x & -\omega_x \\ (\omega-\omega_x)e^{-2i\omega_x} & (\omega+\omega_x)e^{2i\omega_x} \end{pmatrix}\begin{pmatrix} A_1 \\ A_2 \end{pmatrix}=\begin{pmatrix} -i \\ 0 \end{pmatrix}. \tag{5.2}$$

The solution respectively represents propagating modes and evanescent modes when the mode number k is below the cut-off value

$$k \leq k_{\text{cut-off}} = \frac{\omega}{\pi}$$

and up the cut-off value

$$k > k_{\text{cut-off}}.$$

We compute numerical approximations for the highest propagating mode and the lowest evanescent modes. The simulations are performed for the wave number $\omega = 20$ and 40 when the corresponding highest propagating mode numbers are k=6 and 12. The Tables 1-4 below give a comparison of iteration numbers and computing time between two preconditioners, and we list the approximation error for the mode numbers k.

From the Tables 1-4, we can see that, for a fixed k, the iteration number and the computing time of the preconditioned BICGSTAB with the new preconditioner $\mathcal{B}$ increases much more slowly with respect to h than that with the original preconditioner $\mathcal{D}$ proposed in [13]. Moreover, the iteration number and the computing time with the preconditioner $\mathcal{B}$ is significantly less than those with the preconditioner $\mathcal{D}$. Results listed in the Tables 1-2 indicate that the damped Richardson's scheme is completely invalid to solve the underlying linear system. All these show that the new preconditioner $\mathcal{B}$ is much more effective than the original preconditioner $\mathcal{D}$.

The results listed in Table 3 indicate that the choice $d/h = 4$ conduces less computing time than the other choice ($d/h = 3,6$), but the results listed in Table 4 indicate that the choice $d/h = 6$ brings on less computing time than other cases ($d/h = 3,4$). Besides, the iteration number of the choice d/h=6 increases much more slowly with respect to h than that of other cases (d/h=3,4) for ω=20,40. Therefore, when the wave number ω increases and h decreases, the size of subdomain d should decrease with a suitable scaling in order

Table 1: A comparison of iteration numbers and computing time between three strategies for $\omega = 20$.

Methods		$\mathcal{D}$+BICGSTAB			$\mathcal{D}$+ Richardson		
h	k	err.	N_{iter}	$T_{sol}(sec)$	err.	N_{iter}	$T_{sol}(sec)$
$\frac{1}{12}$	6	$2.40e-6$	407	8.01	$5.67e-2$	5000+	31.33
	7	$2.11e-5$	229.5	4.97	$5.89e-2$	5000+	30.14
$\frac{1}{24}$	6	$1.48e-7$	901.5	$7.28e+1$	$1.19e-1$	5000+	$1.58e+2$
	7	$1.04e-6$	478	38.15	$3.36e-1$	5000+	$1.48e+2$

Table 2: A comparison of iteration numbers and computing time between three strategies for $\omega = 40$.

Methods		$\mathcal{D}$+BICGSTAB			$\mathcal{D}$+ Richardson		
h	k	err.	N_{iter}	$T_{sol}(sec)$	err.	N_{iter}	$T_{sol}(sec)$
$\frac{1}{24}$	12	$2.30e-6$	2081	$1.50e+2$	$3.56e-2$	5000+	$1.59e+2$
	13	$4.40e-6$	621	54.88	$6.63e-1$	5000+	$1.49e+2$
$\frac{1}{48}$	12	$1.11e-7$	4685	$1.93e+3$	$1.55e-1$	5000+	$5.65e+2$
	13	$3.32e-6$	1517.5	$6.10e+2$	$7.89e-1$	5000+	$5.15e+2$

Table 3: A comparison of iteration numbers and computing time between three strategies for $\omega=20$.

$\mathcal{B}$+BICGSTAB		err.	$d/h=3$		$d/h=4$		$d/h=6$	
h	k		N_{iter}	$T_{sol}(sec)$	N_{iter}	$T_{sol}(sec)$	N_{iter}	$T_{sol}(sec)$
$\frac{1}{12}$	6	$2.40e-6$	51.5	1.66	56	1.39	87	1.97
	7	$2.11e-5$	52.5	1.77	62.5	1.77	83	1.89
$\frac{1}{24}$	6	$3.61e-8$	78.5	16.25	85	9.56	108	12.63
	7	$3.46e-7$	76	15.88	81.5	9.89	99.5	11.24

Table 4: A comparison of iteration numbers and computing time between three strategies for $\omega=40$.

$\mathcal{B}$+BICGSTAB		err.	$d/h=3$		$d/h=4$		$d/h=6$	
h	k		N_{iter}	$T_{sol}(sec)$	N_{iter}	$T_{sol}(sec)$	N_{iter}	$T_{sol}(sec)$
$\frac{1}{24}$	12	$2.30e-6$	63	13.01	66.5	10.62	98	9.71
	13	$4.40e-6$	52	11.75	62	11.81	85.5	9.00
$\frac{1}{48}$	12	$3.67e-8$	75.5	97.92	81	63.12	116	62.14
	13	$5.81e-8$	73.5	$1.01e+2$	84.5	$6.75e+1$	103	$5.36e+1$

to keep some balance between the iteration counts of $\mathcal{B}$+BICGSTAB and the computing complexity for the coarse solver $\mathcal{A}_d$ (if d is too large, the iteration counts of $\mathcal{B}$+BICGSTAB is great; if d is too small, the cost for implementing $\mathcal{A}_d^{-1}$ is large).

5.2 A two-dimensional singular problem in an L-shaped domain

The second model problem is the following Helmholtz equations (see [21]):

$$\Delta u+\omega^2 u=0, \qquad \text{in } \Omega, \tag{5.3a}$$

$$u=0, \qquad \text{on } \Gamma_1, \tag{5.3b}$$

$$\frac{\partial u}{\partial \mathbf{n}}+i\omega u=\frac{\partial g}{\partial \mathbf{n}}+i\omega g, \qquad \text{on } \partial\Gamma_2, \tag{5.3c}$$

where Ω is an L-shaped domain, which is shown in Fig. 1. The exterior boundary Γ is divided into parts $\Gamma=\Gamma_1+\Gamma_2$ so that the edges meeting at the origin are denoted by Γ_1 and the rest of boundary Γ constitutes Γ_2. Besides we set

$$g(r,\theta)=J_{2/3}(\omega r)\sin\left(\frac{2}{3}\theta\right),$$

so the exact solution of this problem is $u_{ex}=g$. This solution has a singular derivative at the origin (of course $u_{ex}\in H^1(\Omega)$).

In the L-shaped domain example we adopt the uniform mesh (Fig. 1).

From the Tables 5-6, we can see that the new preconditioner $\mathcal{B}$ is also much more effective than the original preconditioner $\mathcal{D}$. In addition, the results listed in Table 6 indicate that the choice $d/h=4$ leads less computing time than the other choices ($d/h=$ 3,6) and the iteration number of the choice $d/h=6$ increases much more slowly with respect to h than that of other cases ($d/h=3,4$) for $\omega=20,40$.

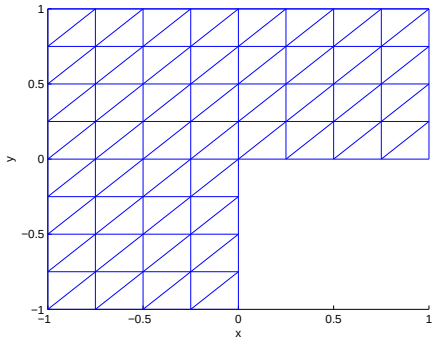

Figure 1: The meshes for the L-shaped domain.

Table 5: A comparison of iteration numbers and computing time between three strategies.

Methods		$\mathcal{D}$+BICGSTAB			$\mathcal{D}$+ Richardson		
ω	h	err.	N_{iter}	$T_{sol}(sec)$	err.	N_{iter}	$T_{sol}(sec)$
20	$\frac{1}{12}$	$2.81e-2$	241.5	2.81	$2.81e-2$	599	1.82
	$\frac{1}{24}$	$1.06e-2$	472.5	$2.29e+1$	$1.06e-2$	1956	$2.37e+1$
40	$\frac{1}{24}$	$2.97e-2$	493.5	$2.41e+1$	$2.97e-2$	1148	$1.46e+1$
	$\frac{1}{48}$	$1.05e-2$	947	$2.05e+2$	$1.05e-2$	2395	$1.20e+2$

Table 6: A comparison of iteration numbers and computing time between three strategies.

$\mathcal{B}$+BiCGSTAB		err.	$d/h=3$		$d/h=4$		$d/h=6$	
ω	h		N_{iter}	$T_{sol}(sec)$	N_{iter}	$T_{sol}(sec)$	N_{iter}	$T_{sol}(sec)$
20	$\frac{1}{12}$	$2.81e-2$	80	$9.97e-1$	113	1.20	171	1.94
	$\frac{1}{24}$	$1.06e-2$	85.5	7.19	104	5.61	145	6.14
40	$\frac{1}{24}$	$2.97e-2$	98.5	5.84	161	8.80	300.5	$1.27e+1$
	$\frac{1}{48}$	$1.05e-2$	81	$3.45e+1$	97	$2.76e+1$	182	$4.61e+1$

5.3 A smooth homogeneous problem in 3D

The third model problem is the following Helmholtz equations

$$\Delta u+\omega^2 u=0, \qquad \text{in } \Omega, \tag{5.4a}$$

$$\frac{\partial u}{\partial \mathbf{n}}+i\omega u=g, \qquad \text{over } \partial\Omega, \tag{5.4b}$$

where $\Omega=[0,1]\times[0,1]\times[0,1]$, and $g=i\omega(1+\vec{v}_0\cdot\mathbf{n})e^{i\omega\vec{v}_0\cdot\vec{x}}$. The exact solution of the problem can be obtained in the closed form as

$$u_{ex}(\vec{x})=e^{i\omega\vec{v}_0\cdot\vec{x}},$$

Table 7: A comparison of iteration numbers and computing time between three strategies.

Methods		$\mathcal{D}$+BICGSTAB			$\mathcal{D}$+ Richardson		
ω	h	err.	N_{iter}	$T_{sol}(sec)$	err.	N_{iter}	$T_{sol}(sec)$
10	$\frac{1}{12}$	$1.43e-4$	114.5	$6.99e+1$	$1.43e-4$	5000+	$4.51e+2$
	$\frac{1}{24}$	$7.21e-6$	228.5	$8.98e+2$	$7.21e-6$	5000+	$3.54e+3$
20	$\frac{1}{12}$	$3.04e-3$	104	$4.95e+1$	$3.04e-3$	302	$2.32e+1$
	$\frac{1}{24}$	$1.22e-4$	203	$7.95e+2$	$1.22e-4$	5000+	$3.65e+3$

Table 8: A comparison of iteration numbers and computing time between three strategies.

$\mathcal{B}$+BICGSTAB		err.	$d/h=4$		$d/h=6$	
ω	h		N_{iter}	$T_{sol}(sec)$	N_{iter}	$T_{sol}(sec)$
10	$\frac{1}{12}$	$1.43e-4$	62	$4.06e+1$	73.5	$4.17e+1$
	$\frac{1}{24}$	$7.21e-6$	76	$3.97e+2$	99.5	$4.72e+2$
20	$\frac{1}{12}$	$3.04e-3$	61.5	$3.27e+1$	93	$4.50e+1$
	$\frac{1}{24}$	$1.22e-4$	55.5	$4.97e+2$	92	$4.29e+2$

where

$$\vec{v_1}=(\tan(-\pi/10),0,\tan(\pi/5))^t,\quad \vec{v_0}=\vec{v_1}/\|\vec{v_1}\|_2.$$

Tables 7-8 below give a comparison of iteration numbers and computing time between three strategies.

We can find that, from the Tables 7-8, that the new preconditioner $\mathcal{B}$ is still much more effective than the original preconditioner $\mathcal{D}$ for three-dimensional problems. In addition, similarly to the 2-D cases, the results listed in Table 8 indicate that, the choice $d/h=4$ induces less computing time than the choice $d/h=6$ for $\omega=10$ and the choice $d/h=6$ induces less computing time than the choice $d/h=4$ for $\omega=20$. Besides, the iteration number of the choice $d/h=4$ increases much more slowly with respect to h than that of the other case ($d/h=6$) for $\omega=10,20$.

The following Fig. 2 describes real part and imaginary part of the exact solution and the numerical solution in the plane z=0.5, respectively. From this figures, we can find that the numerical field, computed using UWVF, is indistinguishable from the exact solution.

5.4 A point source problem

The following test problem consists of a point source (see [22]):

$$u(r,r_0)=\frac{1}{4\pi}\frac{e^{i\omega|r-r_0|}}{|r-r_0|}$$

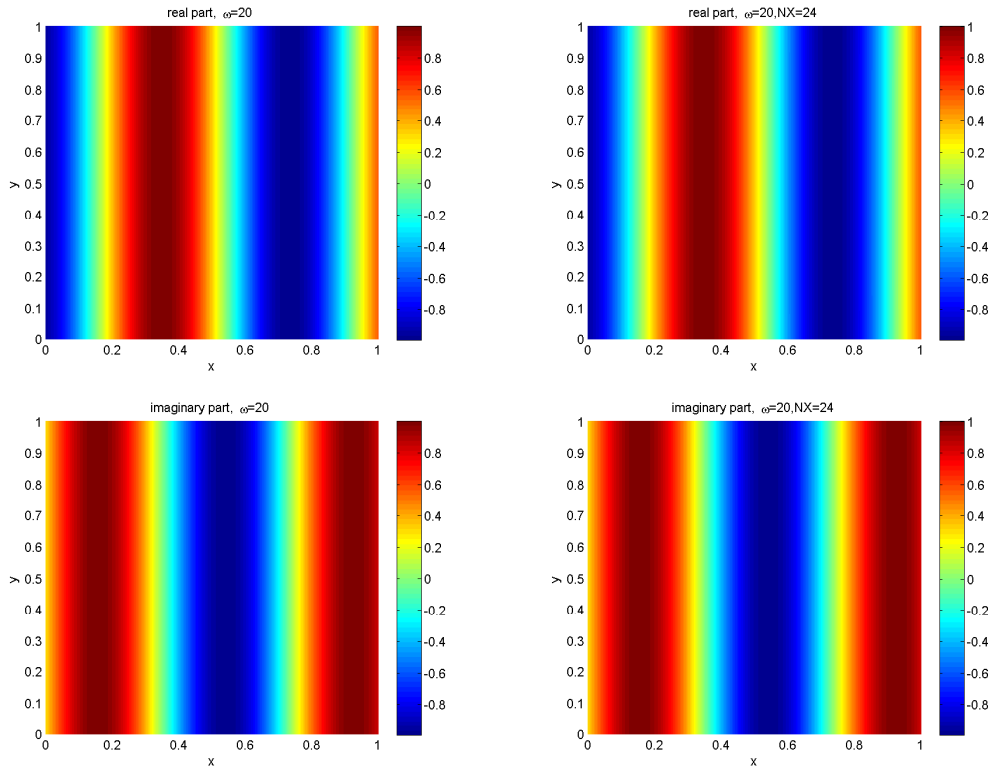

Figure 2: The first row is the real part of the exact solution and the numerical solution. The second row is the imaginary part of the exact solution and the numerical solution.

in a cubic computational domain $\Omega=[-1,1]\times[-1,1]\times[-1,1]$ centred at the origin. The location of the source is off-centred at $r_0=(1,1,1)$ and $r=(x,y,z)$ is an observation point. Tables 9-10 below give a comparison of iteration numbers and computing time between three strategies.

We found from the above table that the iteration number and the computing time of the preconditioned BICGSTAB with the new preconditioner $\mathcal{B}$ increases much more slowly with respect to h than that with the original preconditioner $\mathcal{D}$ proposed in [13]. Moreover, the iteration number and the computing time with the preconditioner $\mathcal{B}$ is significantly less than those with the preconditioner $\mathcal{D}$. In addition, results listed in table 9 indicate that the damped Richardson's scheme is completely invalid to solve the underlying linear system. All these show that the new preconditioner $\mathcal{B}$ is much more effective than the original preconditioner $\mathcal{D}$. In addition, the results listed in Table 10 indicate that, the iteration number and the computing time of the choice $d/h=6$ increases much more slowly with respect to h than that of the choice $d/h=4$.

Fig. 3 describes real part and imaginary part of the exact solution and the numerical solution in the plane $z=0$, respectively. From the above figures, we can find that the numerical field, computed using UWVF, is indistinguishable from the exact solution.

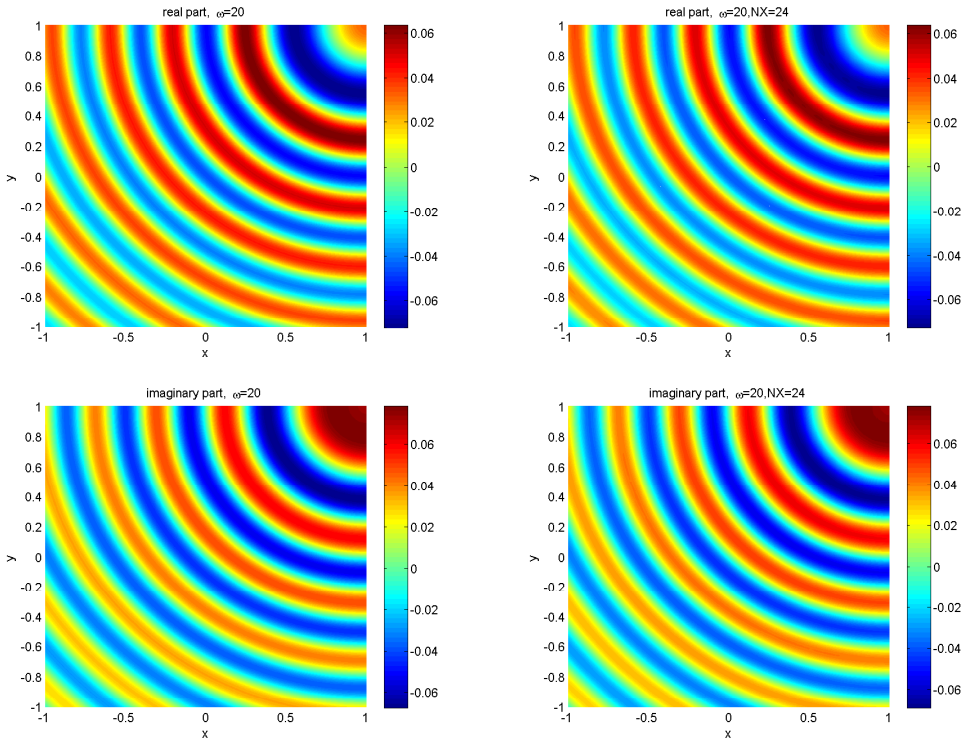

Figure 3: The first row is the real part of the exact solution and the numerical solution. The second row is the imaginary part of the exact solution and the numerical solution.

Table 9: A comparison of iteration numbers and computing time between three strategies.

Methods		$\mathcal{D}$+BiCGSTAB			$\mathcal{D}$+ Richardson		
ω	h	err.	N_{iter}	$T_{sol}(sec)$	err.	N_{iter}	$T_{sol}(sec)$
5	$\frac{1}{6}$	$1.58e-1$	117.5	$5.80e+1$	$1.58e-1$	5000+	$4.16e+2$
	$\frac{1}{12}$	$1.56e-1$	236	$9.85e+2$	$1.56e-1$	5000+	$3.98e+3$
10	$\frac{1}{6}$	$1.19e-1$	111	$5.41e+1$	$1.19e-1$	323	$2.69e+1$
	$\frac{1}{12}$	$1.14e-1$	208.5	$9.01e+2$	$1.14e-1$	5000+	$4.09e+3$

6 Conclusions

We have introduced a new preconditioner for the system arising from the ultra weak variational formulation for both two-dimensional and three-dimensional Helmholtz equations. The effectiveness of the method for the large-scale numerical modelling of acoustic fields was confirmed by some numerical experiments. In comparison with the original preconditioner proposed in [13], the new preconditioner showed significant improvement in both iteration numbers and computing time.

Table 10: A comparison of iteration numbers and computing time between three strategies.

$\mathcal{B}$+BiCGSTAB		err.	$d/h=4$		$d/h=6$	
ω	h		N_{iter}	$T_{sol}(sec)$	N_{iter}	$T_{sol}(sec)$
5	$\frac{1}{6}$	$1.58e-1$	61.5	$4.33e+1$	83	$5.34e+1$
	$\frac{1}{12}$	$1.56e-1$	84	$5.18e+2$	109	$5.15e+2$
10	$\frac{1}{6}$	$1.19e-1$	60.5	$2.68e+1$	84	$3.81e+1$
	$\frac{1}{12}$	$1.14e-1$	65	$4.16e+2$	84	$3.88e+2$

Acknowledgments

The second author was supported by the Major Research Plan of Natural Science Foundation of China G91130015, the Key Project of Natural Science Foundation of China G11031006 and National Basic Research Program of China G2011309702.

References

[1] B. DESPRÉS, Méthod de DÉComposition de Domaine Pour Les Problèmes de Propagation D'Ondes en RÉGime Harmonique, Le théorème de Borg Pour L'Équation de Hill Vectorielle, Ph.D.thesis, FRANCE/Paris IX Dauphine,1991.

[2] C. POTIER AND R. MARTRET, *Finite volume solution of Maxwell's equations in non-steady mode*, La Recherche Aérospatiale, 5 (1994), pp. 329–342.

[3] K. YEE, *Numerical solution of initial boundary value problem in isotropic meida*, IEEE Trans. Antennas Propagation, AP-14 (1966), pp. 302–307.

[4] A. DERAEMAEKER, I. BABUSKA AND P. BOUILLARD, *Dispersion and pollution of the FEM solution for the Helmholtz equation in one, two and three dimensions*, Int. J. Numer. Meth. Eng., 46 (1999), pp. 471–499.

[5] R. FREYMANN, Advanced Numerical and Experimental Methods in the Field of Vehicle Structural acoustics, Hieronymus Buchreproduktions GmbH, München, 2000.

[6] I. HARARI AND T. HUGHES, *Galerkin/least-squares finite element methods for the reduced wave equation with non-reflecting boundary conditions in unbounded domains*, Comput. Meth. Appl. Mech. Eng., 98(3) (1992), pp. 411–454.

[7] I. BABUSKA, F. IHLENBURG, E. PAIK AND S. SAUTER, *A generalized finite element method for solving the helmholtz equation in two dimensions with minimal pollution*, Comput. Meth. Appl. Mech. Eng., 128 (1995), pp. 325–359.

[8] J. MELENK AND I. BABUSKA, *The partition of unity finite element method: Basic theory and applications*, Comput. Meth. Appl. Mech. Eng., 139 (1996), pp. 289–314.

[9] J. MELENK AND I. BABUSKA, *Approximation with harmonic and generalized harmonic polynomials in the partition of unity method*, Comput. Assist. Mech. Eng. Sci., 4 (1997), pp. 607–632.

[10] C. SOIZE, *Reduced models in the medium frequency range for the general dissipative structural dynamic systems*, Euro. J. Mech. A/Solids, 17 (1998), pp. 657–685.

[11] E. LANGRE, *Fonctions de transfert de plaques par équations intégrales, Test de validation et de performance*, Rapport CEA. DMT/90/395 (1991).

[12] I. HARARI AND T. HUGUES, *A cost comparison of boundary element and finite element methods for problems of time-harmonic acoustics*, Comput. Meth. Appl. Mech. Eng., 97 (1992) pp. 77–102.
[13] O. CESSENAT AND B. DESPRES, *Application of an ultra weak variational formulation of elliptic pdes to the two-dimensional helmholtz problem*, SIAM J. Numer. Anal., 35(1) (1998), pp. 255–299.
[14] T. HUTTUNEN, P. MONK AND J. KAIPIO, *Computational aspects of the Ultra-weak variational formulation*, J. Comput. Phys., 182(1) (2002), pp. 27–46.
[15] H. RIOU, P. LADEVÈZE AND B. SOURCIS, *The multiscale VTCR approach applied to acoustics problems*, J. Comput. Acous., 16 (2008), pp. 487–505.
[16] T. HUTTUNEN, M. MALINEN AND P. MONK, *Solving Maxwell's equations using the ultra weak variational formulation*, J. Comput. Phys., 223 (2007), pp. 731–758.
[17] G. OPFER AND G. SCHOBER, *Richardson's iteration for nonsymmetric matrices*, Linear Algebra. Appl., 58 (1984), pp. 343–361.
[18] J. LIONS AND E. MAGENES, *Problèmes aux limites non homogènes et applications*, 1 (1968), et 2, Dunod, Pairs.
[19] R. TEZAUR AND C. FARHAT, *Three-dimensional directional discontinuous Galerkin elements with plane waves and Lagrange multipliers for the solution of mid-frequency Helmholtz problems*, Int. J. Numer. Meth. Eng., 66 (2006), pp. 796–815.
[20] T. HUTTUNEN, P. GAMALLO AND R. ASTLEY, *Comparison of two wave element methods for the Helmholtz problem*, Commun. Numer. Meth. Eng., 25 (2009), pp. 35–52.
[21] T. LUOSTARI, T. HUTTUNEN AND P. MONK, *The ultra weak variational formulation using Bessel basis functions*, Commun. Comput. Phys., 11 (2012), pp. 400–414.
[22] T. HUTTUNEN, J. KAIPIO AND P. MONK, *The perfectly matched layer for the ultra weak variational formulation of the 3D Helmholtz equation*, Int. J. Numer. Meth. Eng., 61 (2004), pp. 1072–1092.
[23] QIYA. HU, XUE-CHENG. TAI AND RAGNAR. WINTHER, *A saddle point approach to the computation of harmonic maps*, SIAM J. Numer. Anal., 47 (2009), pp. 1500–1523.